

Leptonic contribution to the bulk viscosity of nuclear matter

Mark G. Alford and Gerald Good

Physics Department, Washington University, St. Louis, Missouri 63130, USA

(Received 22 March 2010; published 15 November 2010)

For β -equilibrated nuclear matter we estimate the contribution to the bulk viscosity from purely leptonic processes, namely the conversion of electrons to and from muons. For oscillation frequencies in the kilohertz range, we find that this process provides the dominant contribution to the bulk viscosity when the temperature is well below the critical temperature for superconductivity or superfluidity of the nuclear matter.

DOI: [10.1103/PhysRevC.82.055805](https://doi.org/10.1103/PhysRevC.82.055805)

PACS number(s): 26.60.-c, 21.65.Cd, 67.10.Jn

I. INTRODUCTION

The bulk viscosity of nuclear matter plays an important role in the damping of oscillations in neutron stars. One well-known example is r modes, which, if the interior of the star is a perfect (dissipationless) fluid, become unstable with respect to the emission of gravitational waves [1–3]. This emission acts as a brake on the rotation of the star. However, r -mode spindown will not occur if the r mode is sufficiently strongly damped, for example, by shear or bulk viscosity of the matter in the interior of the star. It is therefore important to calculate the bulk viscosity of the various candidate phases in a neutron star. Several calculations exist in the literature, for nuclear [4–9] and hyperonic matter [10–12] as well as for unpaired quark matter [13–15] and various color-superconducting phases [16–21].

In this paper we will study β -equilibrated nuclear matter. We define the chemical potential for charged leptons to be $\mu_l = -\phi/e$, where ϕ is the electrostatic potential and e is the positron charge. We will assume that the density is high enough that μ_l is greater than the mass of the muon, so the matter consists of neutrons, protons, electrons, and muons. Such matter is expected to exist in the core of the star. In previous calculations of bulk viscosity of $npe\mu$ nuclear matter, the focus has been on the contribution from interconversion of neutrons and protons via weak interactions. But nuclear matter at neutron-star densities is expected to show Cooper pairing of protons (superconductivity) or neutrons (superfluidity) [22–24], either of which will suppress interconversion by a factor of order $\exp(-\Delta/T)$, where Δ is the energy gap at the Fermi surface and T is the temperature. This opens up the possibility that, in superfluid or superconducting phases, the dominant contribution to the bulk viscosity might come from purely leptonic processes. The relevant process is conversion of electrons to muons (and vice versa) via either the direct Urca process or the modified Urca process. The direct Urca leptonic conversion process is forbidden by energy and momentum conservation: In converting an electron near its Fermi surface to a muon near its Fermi surface, the change in free energy is very small (of order T), so the emitted neutrinos carry momentum and energy of this order; but the change of momentum of the charged lepton is large, at least $q_{\min} = \mu_l - \sqrt{\mu_l^2 - m_\mu^2}$, and the low-energy neutrino cannot carry this much momentum. However, the modified Urca process can occur; for example, two electrons with energy slightly above the Fermi energy can scatter to an electron and a muon with energies near the Fermi energy, or an electron

and muon can scatter to two muons. The strongest interaction between leptons is electromagnetism, so this process proceeds via exchange of a photon, whose propagator should include the effects of screening by the nuclear medium. As the temperature decreases, the process will become suppressed as the Fermi distributions assume their zero-temperature step function profiles, but at finite temperature the modified Urca process will result in a nonzero contribution to the bulk viscosity. We calculate the leptonic bulk viscosity arising from the processes $e + \ell \rightleftharpoons \mu + \ell + \nu + \bar{\nu}$, where $\ell = e$ or μ . All our calculations are in the “subthermal” regime, where the density oscillation has a small amplitude, and the bulk viscosity is independent of that amplitude. We conclude that, if the protons and neutrons are both ungapped, i.e., if there is neither superfluidity nor superconductivity, then the bulk viscosity from these purely leptonic processes is several orders of magnitude smaller than that from the nucleonic processes. However, once the temperature drops below the critical value for Cooper pairing of the protons or neutrons, the nucleonic bulk viscosity at frequencies $\gtrsim 10$ Hz is strongly suppressed, and leptonic processes become the dominant source of bulk viscosity at those frequencies.

In Sec. II, we lay out the process for calculating the bulk viscosity of a two-component leptonic system under application of a periodic volume and pressure perturbation. A crucial component of this calculation is the conversion rate between electrons and muons, which is discussed in Sec. III. In Sec. IV, we show the numerical results of our calculations and how they compare to the bulk viscosity resulting from modified Urca equilibration of the nucleon population.

II. BULK VISCOSITY OF LEPTONS

First we write down a general expression for bulk viscosity in a two-species system, arising from interconversion of the two species. Then we specialize to the case of electrons and muons in nuclear matter.

A. Bulk viscosity of a two-species system

We assume that the system experiences a small-amplitude driving oscillation

$$\begin{aligned} V(t) &= \bar{V} + \text{Re}(\delta V e^{i\omega t}), \\ p(t) &= \bar{p} + \text{Re}(\delta p e^{i\omega t}), \end{aligned} \quad (1)$$

where the volume amplitude $\delta V \ll \bar{V}$ is real by convention, and the resultant pressure oscillation $p(t)$ is complex. The average power dissipated per unit volume is

$$\frac{dE}{dt} = -\frac{1}{\tau \bar{V}} \int_0^\tau p(t) \frac{dV}{dt} dt = -\frac{1}{2} \omega \text{Im}(\delta p) \frac{\delta V}{\bar{V}}, \quad (2)$$

where $\tau = 2\pi/\omega$, so the bulk viscosity is [14]

$$\zeta = \frac{2\bar{V}^2}{\omega^2(\delta V)^2} \frac{dE}{dt} = -\frac{\text{Im}(\delta p) \bar{V}}{\delta V \omega}. \quad (3)$$

We will determine $\text{Im}(\delta p)$, which will be negative. We will assume that heat arising from dissipation is conducted away quickly, so the whole calculation is performed at constant temperature T . We assume that our system contains two particle species e and μ , and the state of the system is determined by the corresponding chemical potentials μ_e and μ_μ . The total number of electrons and muons is conserved, and equilibrium is established via the conversion process $e \leftrightarrow \mu$. For simplicity of presentation and of the final expressions, it is better to work in terms of charged lepton number l and electron-muon asymmetry a , so pressure is a function of μ_l and μ_a , where

$$\begin{aligned} \mu_l &= \frac{1}{2}(\mu_e + \mu_\mu), & n_l &= n_e + n_\mu = \left. \frac{\partial p}{\partial \mu_l} \right|_{\mu_a}, \\ \mu_a &= \frac{1}{2}(\mu_e - \mu_\mu), & n_a &= n_e - n_\mu = \left. \frac{\partial p}{\partial \mu_a} \right|_{\mu_l}. \end{aligned} \quad (4)$$

From now on all partial derivatives with respect to μ_l will be assumed to be at constant μ_a , and vice versa. In β equilibrium, μ_a is zero. The variations in the chemical potentials are expressed in terms of complex amplitudes $\delta\mu_l$ and $\delta\mu_a$,

$$\begin{aligned} \mu_l(t) &= \bar{\mu}_l + \text{Re}(\delta\mu_l e^{i\omega t}), \\ \mu_a(t) &= \text{Re}(\delta\mu_a e^{i\omega t}). \end{aligned} \quad (5)$$

The pressure amplitude is then

$$\delta p = \left. \frac{\partial p}{\partial \mu_l} \right|_{\mu_a} \delta\mu_l + \left. \frac{\partial p}{\partial \mu_a} \right|_{\mu_l} \delta\mu_a = n_l \delta\mu_l + n_a \delta\mu_a. \quad (6)$$

From Eqs. (6) and (3) we find

$$\zeta = -\frac{1}{\omega} \frac{\bar{V}}{\delta V} [\bar{n}_l \text{Im}(\delta\mu_l) + \bar{n}_a \text{Im}(\delta\mu_a)]. \quad (7)$$

To obtain the imaginary parts of the chemical potential amplitudes, we write down the rate of change of the corresponding conserved quantities,

$$\begin{aligned} \frac{dn_l}{dt} &= \frac{\partial n_l}{\partial \mu_l} \frac{d\mu_l}{dt} + \frac{\partial n_l}{\partial \mu_a} \frac{d\mu_a}{dt} = -\frac{n_l}{\bar{V}} \frac{dV}{dt}, \\ \frac{dn_a}{dt} &= \frac{\partial n_a}{\partial \mu_l} \frac{d\mu_l}{dt} + \frac{\partial n_a}{\partial \mu_a} \frac{d\mu_a}{dt} = -\frac{n_a}{\bar{V}} \frac{dV}{dt} - \Gamma_{e \rightarrow \mu}^{\text{total}}. \end{aligned} \quad (8)$$

All the partial derivatives are evaluated at equilibrium, $\mu_l = \bar{\mu}_l$ and $\mu_a = 0$. The right-hand term on the first line of Eq. (8) expresses the fact that charge is conserved, so when a volume is compressed, the density of charged leptons rises. On the second line of Eq. (8), there is such a term from the compression of the existing population of particles, but there is also a rate of conversion $\Gamma_{e \rightarrow \mu}^{\text{total}}$ of electrons to muons, which

reflects the fact that weak interactions will push the lepton densities toward their equilibrium value. For small deviations from equilibrium we expect $\Gamma_{e \rightarrow \mu}^{\text{total}}$ to be linear in μ_a , so it is convenient to write the rate in terms of an average width γ_a , which is defined in terms of the total rate by writing

$$\Gamma_{e \rightarrow \mu}^{\text{total}} = \gamma_a \frac{\partial n_a}{\partial \mu_a} \mu_a. \quad (9)$$

We now substitute the assumed oscillations (1) and (5) into Eq. (8), and solve to obtain the amplitudes $\delta\mu_l$ and $\delta\mu_a$ in terms of the amplitude δV and frequency ω of the driving oscillation. Inserting their imaginary parts in Eq. (7) we obtain the bulk viscosity, which is conveniently expressed in terms of the susceptibilities

$$\begin{aligned} \chi_{ll} &= \frac{\partial n_l}{\partial \mu_l}, \\ \chi_{la} &= \frac{\partial n_l}{\partial \mu_a} = \frac{\partial n_a}{\partial \mu_l}, \\ \chi_{aa} &= \frac{\partial n_a}{\partial \mu_a}, \end{aligned} \quad (10)$$

all evaluated at equilibrium, $\mu_l = \bar{\mu}_l$, $\mu_a = 0$. Note that χ_{al} is the same as χ_{la} from Eq. (4). Defining

$$\begin{aligned} \gamma_{\text{eff}} &= \frac{\chi_{ll} \chi_{aa}}{\chi_{ll} \chi_{aa} - \chi_{la}^2} \gamma_a = \frac{\chi_{ll}}{\chi_{ll} \chi_{aa} - \chi_{la}^2} \left. \frac{\partial \Gamma_{e \rightarrow \mu}^{\text{total}}}{\partial \mu_a} \right|_{\mu_a=0}, \\ C &= \frac{(\chi_{ll} n_a - \chi_{la} n_l)^2}{\chi_{ll} (\chi_{ll} \chi_{aa} - \chi_{la}^2)}, \end{aligned} \quad (11)$$

we obtain the final result for the bulk viscosity in a two-species system,

$$\zeta = C \frac{\gamma_{\text{eff}}}{\omega^2 + \gamma_{\text{eff}}^2}. \quad (12)$$

From Eq. (12) we can already see how the bulk viscosity of a two-species system depends on the frequency ω of the oscillation and the effective equilibration rate γ_{eff} .

At fixed equilibration rate, the bulk viscosity decreases monotonically as the oscillation frequency rises; it is roughly constant for $\omega \lesssim \gamma_{\text{eff}}$, and then drops off quickly as $1/\omega^2$ for $\omega \gg \gamma_{\text{eff}}$.

At fixed oscillation frequency ω , the bulk viscosity is a nonmonotonic function of the rate γ_{eff} . It is peaked at $\gamma_{\text{eff}} = \omega$, with a value of

$$\zeta_{\text{max}} = \frac{1}{2} C / \omega. \quad (13)$$

For $\gamma_{\text{eff}} \ll \omega$ or $\gamma_{\text{eff}} \gg \omega$, the bulk viscosity tends to zero. Thus, very fast and very slow processes are not an important source of bulk viscosity. As we will see below, for leptons in nuclear matter, the equilibration rate is sensitive to temperature but the coefficient C is not, so we expect $\zeta(T)$ to be peaked at $\gamma_{\text{eff}}(T) = \omega$, where the oscillation frequency ω is of the order of kilohertz for typical oscillation modes of neutron stars.

B. Leptons in nuclear matter

In nuclear matter the leptonic chemical potential $\mu_l = \mu_e = \mu_\mu$ is much greater than the temperature and the electron mass, so we can evaluate the susceptibilities (10) at $m_e = T = 0$. Temperature dependence will come in only via the equilibration rate γ_a . Treating the electrons and muons as free fermions, we find

$$\gamma_{\text{eff}} = \gamma_a \frac{(\mu_l + k_F)^2}{4\mu_l k_F}, \quad (14)$$

$$C = \frac{1}{9\pi^2} m_\mu^2 k_F (\mu_l - k_F),$$

where the muon Fermi momentum is given by $k_F^2 = \mu_l^2 - m_\mu^2$. Note that the bulk viscosity goes to zero as $m_\mu \rightarrow 0$ ($m_\mu \rightarrow m_e$, really). This is because, if the muons and electrons have equal mass, then under compression their relative densities do not change, and there is no need for any equilibrating process, so the pressure is always in phase with the volume and no dissipation occurs.

Even without calculating the rate of lepton number equilibration, we can now estimate the amount of bulk viscosity that could possibly arise from leptons. If the equilibrating weak interaction at some temperature happened to have a rate that matched the typical oscillation frequency of the star, $\omega \approx 2\pi \times 1000$ Hz, and the lepton chemical potential had a relatively moderate value of ~ 120 MeV, we would obtain from Eq. (13), $\zeta_{\text{max}} = 5.5 \times 10^{22} \text{ MeV}^3 = 7.5 \times 10^{27} \text{ g s}^{-1} \text{ cm}^{-1}$. This is at the upper end of typical nuclear bulk viscosities, which range up to $10^{28} \text{ g s}^{-1} \text{ cm}^{-1}$ [4]. This motivates us to proceed with the calculation of the rate of conversion of muons to and from electrons via the weak interaction.

III. MUON-ELECTRON CONVERSION RATE

The muon-electron conversion rate $\Gamma_{e \rightarrow \mu}^{\text{total}}$ consists of two partial rates,

$$\Gamma_{e \rightarrow \mu}^{\text{total}} = \Gamma_{ee \rightarrow e\mu}^{\text{total}} + \Gamma_{e\mu \rightarrow \mu\mu}^{\text{total}}. \quad (15)$$

The partial rates are

$$\Gamma_{ab \rightarrow cd}^{\text{total}} = \int \frac{d^3 p_1 d^3 p_2 d^3 p_3 d^3 p_4 d^3 k_1 d^3 k_2}{64(2\pi)^{14} \omega_1 \omega_2 \omega_3 \omega_4 \Omega_1 \Omega_2} \times \delta^4(p_1 + p_2 - p_3 - p_4 - k_1 - k_2) \times W_{ab \rightarrow cd}(p_1 p_2 \rightarrow p_3 p_4 k_1 k_2) \times \{f_a(\omega_1) f_b(\omega_2) [1 - f_c(\omega_3)] [1 - f_d(\omega_4)] - f_c(\omega_1) f_d(\omega_2) [1 - f_a(\omega_3)] [1 - f_b(\omega_4)]\}, \quad (16)$$

where a, b, c, d are either e or μ , and $W_{ab \rightarrow cd}$ is the spin-summed and -averaged matrix element. The charged lepton of flavor j has energy $\omega_j = \sqrt{\mathbf{p}_j^2 + m_j^2}$, the neutrino of flavor j has energy $\Omega_j = |k_j|$, and $f_b(\omega_j)$ is the Fermi distribution function

$$f_b(\omega_j) = \left[1 + \exp\left(\frac{\omega_j - \mu_b}{T}\right) \right]^{-1}. \quad (17)$$

Using the previous definitions for μ_l and μ_a , we have

$$\mu_e = \mu_l + \mu_a, \quad \mu_\mu = \mu_l - \mu_a, \quad (18)$$

and because μ_a is small, to first order in μ_a we have

$$f_e(\omega_1) f_e(\omega_2) [1 - f_e(\omega_3)] [1 - f_\mu(\omega_4)] - f_e(\omega_1) f_\mu(\omega_2) \times [1 - f_e(\omega_3)] [1 - f_e(\omega_4)] = F(\omega_1, \omega_2, \omega_3, \omega_4) \frac{\mu_a}{T} \quad (19)$$

and

$$f_\mu(\omega_1) f_e(\omega_2) [1 - f_\mu(\omega_3)] [1 - f_\mu(\omega_4)] - f_\mu(\omega_1) f_\mu(\omega_2) [1 - f_\mu(\omega_3)] [1 - f_e(\omega_4)] = F(\omega_1, \omega_2, \omega_3, \omega_4) \frac{\mu_a}{T}, \quad (20)$$

$$F(\omega_1, \omega_2, \omega_3, \omega_4) \equiv \frac{2 \exp[(\omega_3 + \omega_4 - 2\mu_l)/T] \{1 + 2 \exp[(\omega_2 - \mu_l)/T] + \exp[(\omega_2 + \omega_4 - 2\mu_l)/T]\}}{\{1 + \exp[(\omega_1 - \mu_l)/T]\} \{1 + \exp[(\omega_2 - \mu_l)/T]\}^2 \{1 + \exp[(\omega_3 - \mu_l)/T]\} \{1 + \exp[(\omega_4 - \mu_l)/T]\}^2}. \quad (21)$$

To determine the content of the matrix elements, we draw the Feynman diagrams for each possible way the reaction can occur. We can draw two different diagrams for each process, depending on whether the weak conversion of the electron to muon occurs before the electromagnetic scattering, or in the reverse order (Figs. 1 and 2). However,

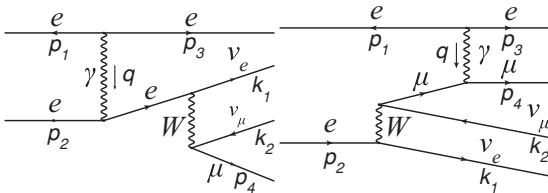


FIG. 1. Feynman diagrams for the process $e + e \rightarrow e + \mu + \bar{\nu}_\mu + \nu_e$. There are an additional two diagrams that are obtained from these by exchanging $p_1 \leftrightarrow p_2$.

because there are identical particles involved, and we are integrating over all initial and final momenta, we need to add two additional diagrams for each process. For the process $e + e \rightleftharpoons \mu + e + \bar{\nu} + \bar{\nu}$, we must add two diagrams where the labels on the initial state electron momenta are reversed; and for the process $e + \mu \rightleftharpoons \mu + \mu + \bar{\nu} + \bar{\nu}$, we must add two

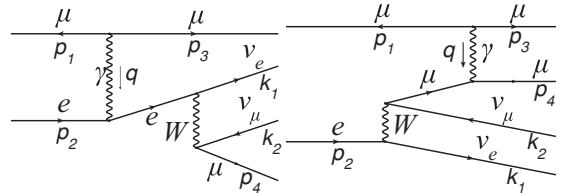


FIG. 2. Feynman diagrams for the process $e + \mu \rightarrow \mu + \mu + \bar{\nu}_\mu + \nu_e$. There are an additional two diagrams that are obtained from these by exchanging $p_3 \leftrightarrow p_4$.

diagrams where the labels on the final state muon momenta are reversed. These diagrams get an additional negative sign for the interchange of fermions [25]. For similar calculations, see Refs. [26] and [27].

Since we have four diagrams for each process, the spin-summed and -averaged matrix elements are

$$W_{ee \rightarrow e\mu} = \frac{1}{8} \sum_{\text{spins}} |E_1 + E_2 - E_3 - E_4|^2, \quad (22)$$

$$W_{e\mu \rightarrow \mu\mu} = \frac{1}{8} \sum_{\text{spins}} |M_1 + M_2 - M_3 - M_4|^2.$$

Here E_1, E_2, E_3, E_4 are the amplitudes corresponding to the diagrams of Fig. 1, and M_1, M_2, M_3, M_4 are the amplitudes corresponding to the diagrams of Fig. 2 [28]:

$$E_1 = \frac{e^2 G_F}{\sqrt{2}(q^2 - q_s^2)} \bar{e}(p_3) \gamma^\mu e(p_1) \bar{\nu}_e(k_1) \gamma^\lambda (1 - \gamma^5) \times \frac{\not{p}_2 + \not{q} + m_e}{(p_2 + q)^2 - m_e^2} \gamma_\mu e(p_2) \bar{\mu}(p_4) \gamma_\lambda (1 - \gamma^5) \nu_\mu(k_2),$$

$$E_2 = \frac{e^2 G_F}{\sqrt{2}(q^2 - q_s^2)} \bar{e}(p_3) \gamma^\mu e(p_1) \bar{\nu}_e(k_1) \gamma^\lambda (1 - \gamma^5) \times e(p_2) \bar{\mu}(p_4) \gamma_\mu \frac{\not{p}_4 - \not{q} + m_\mu}{(p_4 - q)^2 - m_\mu^2} \gamma_\lambda (1 - \gamma^5) \nu_\mu(k_2),$$

$$E_3 = \frac{e^2 G_F}{\sqrt{2}(w^2 - q_s^2)} \bar{e}(p_3) \gamma^\mu e(p_2) \bar{\nu}_e(k_1) \gamma^\lambda (1 - \gamma^5) \times \frac{\not{p}_1 + \not{w} + m_e}{(p_1 + w)^2 - m_e^2} \gamma_\mu e(p_1) \bar{\mu}(p_4) \gamma_\lambda (1 - \gamma^5) \nu_\mu(k_2),$$

$$E_4 = \frac{e^2 G_F}{\sqrt{2}(w^2 - q_s^2)} \bar{e}(p_3) \gamma^\mu e(p_2) \bar{\nu}_e(k_1) \gamma^\lambda (1 - \gamma^5) e(p_1) \times \bar{\mu}(p_4) \gamma_\mu \frac{\not{p}_4 - \not{w} + m_\mu}{(p_4 - w)^2 - m_\mu^2} \gamma_\lambda (1 - \gamma^5) \nu_\mu(k_2), \quad (23)$$

$$M_1 = \frac{e^2 G_F}{\sqrt{2}(q^2 - q_s^2)} \bar{\mu}(p_3) \gamma^\mu \mu(p_1) \bar{\nu}_e(k_1) \gamma^\lambda (1 - \gamma^5) \times \frac{\not{p}_2 + \not{q} + m_e}{(p_2 + q)^2 - m_e^2} \gamma_\mu e(p_2) \bar{\mu}(p_4) \gamma_\lambda (1 - \gamma^5) \nu_\mu(k_2),$$

$$M_2 = \frac{e^2 G_F}{\sqrt{2}(q^2 - q_s^2)} \bar{\mu}(p_3) \gamma^\mu \mu(p_1) \bar{\nu}_e(k_1) \gamma^\lambda (1 - \gamma^5) \times e(p_2) \bar{\mu}(p_4) \gamma_\mu \frac{\not{p}_4 - \not{q} + m_\mu}{(p_4 - q)^2 - m_\mu^2} \gamma_\lambda (1 - \gamma^5) \nu_\mu(k_2),$$

$$M_3 = \frac{e^2 G_F}{\sqrt{2}(s^2 - q_s^2)} \bar{\mu}(p_4) \gamma^\mu \mu(p_1) \bar{\nu}_e(k_1) \gamma^\lambda (1 - \gamma^5) \times \frac{\not{p}_2 + \not{s} + m_e}{(p_2 + s)^2 - m_e^2} \gamma_\mu e(p_2) \bar{\mu}(p_3) \gamma_\lambda (1 - \gamma^5) \nu_\mu(k_2),$$

$$M_4 = \frac{e^2 G_F}{\sqrt{2}(s^2 - q_s^2)} \bar{\mu}(p_4) \gamma^\mu \mu(p_1) \bar{\nu}_e(k_1) \gamma^\lambda (1 - \gamma^5) e(p_2) \times \bar{\mu}(p_3) \gamma_\mu \frac{\not{p}_3 - \not{s} + m_\mu}{(p_3 - s)^2 - m_\mu^2} \gamma_\lambda (1 - \gamma^5) \nu_\mu(k_2), \quad (24)$$

where $w = p_2 - p_3$, and $s = p_1 - p_4$.

The only parameter in our calculation that depends on details of the baryonic matter in the neutron star is the plasma screening momentum q_s . In a full treatment one would have to use the appropriate in-medium propagator, which is a complicated function of the photon momentum.

In this paper we simplify greatly the calculation by assuming that the longitudinal and transverse photons have a common screening mass

$$q_s^2 = 5\alpha\mu_l^2. \quad (25)$$

We argue in Appendix A that this leads to an estimate of the bulk viscosity that is correct to within an order of magnitude at reasonable densities for nuclear matter. As a further test, we also performed calculations with no screening at all ($q_s^2 = 0$), and found that the bulk viscosity shifted by no more than one order of magnitude.

To obtain the equilibration rates, we first multiply out the right-hand sides of Eq. (22) and define partial matrix elements by

$$W_{ee \rightarrow e\mu} = \sum_{i,j \leq i} W_{ee \rightarrow e\mu}^{ij}, \quad W_{e\mu \rightarrow \mu\mu} = \sum_{i,j \leq i} W_{e\mu \rightarrow \mu\mu}^{ij},$$

$$W_{ee \rightarrow e\mu}^{11} = \frac{1}{8} \sum_{\text{spins}} |E_1|^2, \quad W_{ee \rightarrow e\mu}^{12} = \frac{1}{8} \sum_{\text{spins}} (E_1^\dagger E_2 + E_2^\dagger E_1),$$

$$W_{ee \rightarrow e\mu}^{13} = -\frac{1}{8} \sum_{\text{spins}} (E_1^\dagger E_3 + E_3^\dagger E_1), \quad \text{etc.} \quad (26)$$

The traces resulting from the spin sums are easily evaluated with a computer algebra package; we used the FEYNCALC package for MATHEMATICA [29]. In the next few paragraphs, we will describe the steps used to analytically integrate 10 of the 18 integrals, and list the expressions that we subsequently integrated numerically in Appendix B.

We make use of the fact that the neutrino energies are $\sim T \ll \mu_e, \mu_\mu$ by approximating the momentum- and energy-conserving δ functions as

$$\delta^4(p_1 + p_2 - p_3 - p_4 - k_1 - k_2) \approx \delta(\omega_1 + \omega_2 - \omega_3 - \omega_4 - \Omega_1 - \Omega_2) \times \delta^3(\mathbf{p}_1 + \mathbf{p}_2 - \mathbf{p}_3 - \mathbf{p}_4). \quad (27)$$

We then note that k_1 and k_2 occur exactly once in each term, dotted into one of the other four-momenta p_i . Writing

$$k_j = \Omega_j(1, \sin \xi_j \cos \eta_j, \sin \xi_j \sin \eta_j, \cos \xi_j), \quad (28)$$

we can see that any dot product with another four-momentum p_i is

$$p_i \cdot k_j = \Omega_j [\omega_i - (p_i)_x \sin \xi_j \cos \eta_j - (p_i)_y \sin \xi_j \sin \eta_j - (p_i)_z \cos \xi_j]. \quad (29)$$

The integrals over the k_1 and k_2 angular variables then become trivial:

$$\int \frac{d^3 k_j}{\Omega_j} p_i \cdot k_j = \int k_j^2 dk_j d(\cos \xi_j) d\eta_j p_i \cdot \hat{k}_j = 4\pi \omega_i \int_0^\infty \Omega_j^2 d\Omega_j, \quad (30)$$

because all of the integrations over one of the angles ξ_j or η_j are zero.

The energy-momentum-conserving δ function allows us to use relations such as $p_1 - p_3 = p_4 - p_2$ to rewrite some of the denominators of the matrix elements. For example, in $W_{ee \rightarrow e\mu}$ we can substitute variables so that p_3 does not appear in the denominators of any of the terms; then we can integrate out the p_3 three-momentum variables easily. Similarly, in $W_{e\mu \rightarrow \mu\mu}$ we can substitute variables so that p_2 does not appear in the denominators and integrate out the p_2 three-momentum variables. However, our matrix elements have many terms containing the four-momentum p_3 (p_2), so it would be easier if we could integrate over $d^4 p_3$ ($d^4 p_2$). This is accomplished by replacing

$$\begin{aligned} \int \frac{d^3 p_3}{\omega_3} &= \int \frac{d^4 p_3}{(p_3)_0} \delta[(p_3)_0 - \sqrt{\mathbf{p}_3^2 + m_\mu^2}] \\ &\approx \int \frac{d^4 p_3}{(p_3)_0} \delta[(p_3)_0 - \mu_l] \end{aligned} \quad (31)$$

in $W_{ee \rightarrow e\mu}$ and similarly for p_2 in $W_{e\mu \rightarrow \mu\mu}$. In the last approximation we are using the fact that the Fermi distribution function is sharply peaked at low temperatures. Then we integrate over $d^4 p_3$ ($d^4 p_2$) using four of the δ functions.

We can further approximate that the medium is isotropic, by taking one of the remaining momentum variables to be in a fixed direction (the z axis for convenience). The electrons are relativistic, so $\omega_i = |\mathbf{p}_i|$ and $d^3 p_i = \omega_i^2 d\omega_i d\cos\theta_i d\phi_i$ when particle i is an electron. The muons may not be relativistic, so $\omega_i = \sqrt{\mathbf{p}_i^2 + m_\mu^2}$ and $d^3 p_i = \omega_i \sqrt{\omega_i^2 - m_\mu^2} d\omega_i d\cos\theta_i d\phi_i$ when particle i is a muon. We then use the remaining δ function to integrate over the magnitude of this isotropic momentum variable.

The remainder of the integrations are performed numerically. The only further approximation made was to, again, take advantage of the sharply peaked Fermi distribution function, and set $\omega_i = \mu_l$ everywhere inside the integral, except for inside the Fermi function itself. This allows a separation of the eight-dimensional integral into a four-dimensional energy integral and a four-dimensional integral over the angular variables. The integration variables are also changed to dimensionless variables by scaling them with respect to μ_l .

The final expression for each term in the rate has the form

$$\Gamma_{e\ell \rightarrow \mu\ell}^{ij} = \frac{e^4 G_F^2 \mu_l^{12}}{128\pi^{11} m_\mu^4} \left(\frac{\mu_a}{T}\right) \times I_\omega^\ell \times I_{d\Omega}^{ij}, \quad (32)$$

where ℓ is the species of the spectator lepton, and I_ω^ℓ and $I_{d\Omega}^{ij}$ are dimensionless energy and angular integrals, respectively. These integrals are listed in Appendix B.

IV. NUMERICAL RESULTS AND CONCLUSIONS

The remaining part of the rate calculation is performed numerically. The dimensionless energy integrals are nearly the same; a power-law fit of the results yields

$$I_\omega^e \approx 78.86 \left(\frac{T}{\mu_l}\right)^8, \quad I_\omega^\mu \approx 78.62 \left(\frac{T}{\mu_l}\right)^8. \quad (33)$$

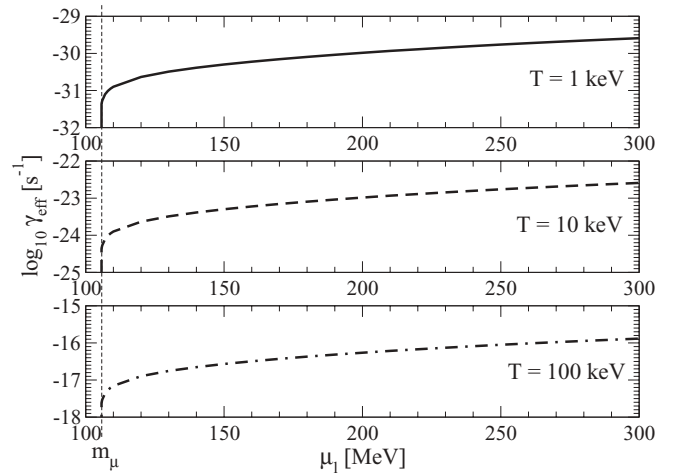


FIG. 3. Dependence of the effective rate of electron-muon conversion γ_{eff} [see Eq. (11)] on the charged-lepton chemical potential μ_l at three different temperatures. As μ_l drops toward m_μ , the muon population decreases and the conversion rate drops to zero. The temperature dependence is T^7 , hence γ_{eff} is much larger at higher temperatures.

In our approximation, the angular integrals only have dependence on μ_l . We determined an analytical fit for the μ_l dependence of $I_{d\Omega}^{eij}$ and $I_{d\Omega}^{\mu ij}$ (accurate within 5%) over the range $120 \text{ MeV} < \mu_l < 300 \text{ MeV}$ by curve fitting the numerical data with sixth-order polynomials:

$$\begin{aligned} \sum_{ij} I_{d\Omega}^{eij} &\approx \left(1 - \frac{m_\mu^2}{\mu_l^2}\right)^{1/2} \sum_{i=0}^6 c_i \left(\frac{\mu_l}{m_\mu}\right)^i, \\ c_0 &= -1.7363 \times 10^4, c_1 = 5.0189 \times 10^4, \\ c_2 &= -4.7644 \times 10^4, c_3 = 1.3224 \times 10^4, \\ c_4 &= 4.4203 \times 10^3, c_5 = -2.7199 \times 10^3, \\ c_6 &= 3.5119 \times 10^2, \end{aligned} \quad (34)$$

$$\begin{aligned} \sum_{ij} I_{d\Omega}^{\mu ij} &\approx \left(1 - \frac{m_\mu^2}{\mu_l^2}\right)^{3/2} \sum_{i=0}^6 c_i \left(\frac{\mu_l}{m_\mu}\right)^i, \\ c_0 &= 1.2433 \times 10^6, c_1 = -3.6329 \times 10^6, \\ c_2 &= 4.4365 \times 10^6, c_3 = -2.8702 \times 10^6, \\ c_4 &= 1.0354 \times 10^6, c_5 = -1.9728 \times 10^5, \\ c_6 &= 1.5507 \times 10^4. \end{aligned} \quad (35)$$

Figure 3 shows the μ_l dependence of the effective rate γ_{eff} defined in Eq. (11). As μ_l approaches m_μ , the rate quickly drops to zero as the muon population disappears. The overall T^7 dependence is also illustrated in the sizable difference in order of magnitude of the rate for the three different temperatures.

Figure 4 shows the temperature dependence of the leptonic bulk viscosity ζ as defined in Eq. (12) for an oscillation frequency $\omega = 2\pi \times 1 \text{ kHz}$. The three approximately straight lines on the log-log plot illustrate the power-law dependence on T for three different values of μ_l . Also plotted are dotted curves showing the nucleonic bulk viscosity for two different values of the critical temperature T_c . These are obtained from

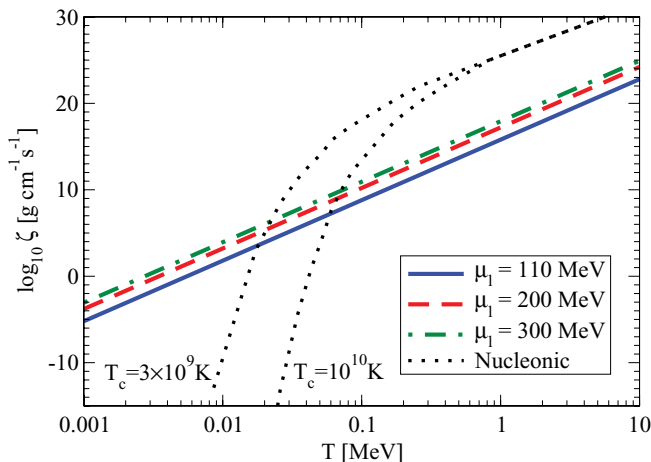


FIG. 4. (Color online) Dependence of the leptonic bulk viscosity ζ on temperature for three different values of the lepton chemical potential, and an oscillation frequency of 1 kHz; for frequency dependence, see the discussion after Eq. (36). We also show the nucleonic bulk viscosity [5] due to modified Urca processes, for two values of the critical temperature.

Ref. [5] in a model where the neutrons are superfluid, pairing in the spin triplet state, the protons are superconducting, pairing in the spin singlet state, and they have a common critical temperature $T_c = T_{cp} = T_{cn}$. Also, it is assumed that only modified Urca processes are available for damping of pulsations (although direct Urca processes would become possible at higher densities). Above the critical temperature for superfluidity-superfluidity, the bulk viscosity for 1 kHz oscillations owing to leptons is several orders of magnitude less than the bulk viscosity owing to nucleons. Below the critical temperature, the nucleonic bulk viscosity quickly decreases, and at a low enough temperature, the leptonic contribution becomes dominant. Based on our calculations, this crossover temperature appears to be of order 0.01–0.1 MeV (10^8 – 10^9 K) for an oscillation frequency in the kilohertz range. Such a suppression of the nucleonic contribution can arise either from superfluidity of neutrons or from superconductivity of protons. Therefore, it is quite possible that, for many cold neutron stars, the bulk viscosity of the superconducting or superfluid region comes mainly from leptonic processes. In regions that are neither superconducting nor superfluid (more strictly, where $T \gtrsim T_{cp}$ and $T \gtrsim T_{cn}$) the nucleonic bulk viscosity will likely dominate.

The viscosity curves in Fig. 4 all slope upward because the equilibration rate $\gamma_{\text{eff}}(T)$ is well below the oscillation frequency ω , so we are in the slow-equilibration (high-frequency) regime of Eq. (12), where

$$\zeta \approx C \frac{\gamma_{\text{eff}}(T)}{\omega^2}. \quad (36)$$

This is true for both leptonic and nuclear viscosities. In this regime one can simply add the two bulk viscosities to get the total bulk viscosity (see, for example, Appendix A of Ref. [17]). As the temperature rises, the equilibration rate and hence the bulk viscosity rise. When $\gamma_{\text{eff}}(T)$ comes close to ω , Eq. (36) becomes a poor approximation to Eq. (12):

ζ reaches a maximum when $\gamma_{\text{eff}}(T) = \omega$. Those maxima, for both leptonic and nuclear bulk viscosities, are beyond the right-hand limit of Fig. 4; for $\mu_l = 200$ MeV, the peak occurs at $T \approx 40$ MeV.

We can now see how our results depend on the frequency of the oscillations. Decreasing ω moves each $\zeta(T)$ curve to the left, shifting the viscosity curves in Fig. 4 upward. The largest value we find for the leptonic effective rate (at $T = 10$ MeV, for $\mu_l = 300$ MeV) is $\gamma_{\text{eff}} \sim 2$ rad/s, so for the leptonic bulk viscosity Eq. (36) is valid for oscillation frequencies well above this value. For example, if we reduced the oscillation frequency from 1000 to 100 Hz, then all the viscosity curves in Fig. 4 would be shifted upward by a factor of 100. Decreasing the frequency still further would bring us to the regime where, in the temperature range of interest, either the nuclear or leptonic rate was comparable to the oscillation frequency (so one or both bulk viscosity curves would show a resonant peak in our plot). Then one may not be able to simply add the bulk viscosities. At extremely low oscillation frequencies, both peaks would shift to very low temperatures, the bulk viscosity curves in our plot would all slope downward, the nucleonic contribution would dominate, and the bulk viscosities could again be added.

It will be interesting to see whether the leptonic contribution that we have calculated here has any impact on oscillations of neutron stars. In the case of r modes, shear viscosity becomes the dominant source of damping in the low-temperature regime, so the leptonic contributions to the bulk viscosity at low temperature are not likely to be an important source of r -mode damping. Also the shear viscosity η of superfluid nuclear matter is much larger than the leptonic bulk viscosity we have calculated: $\eta \sim 10^{16} \text{g cm}^{-1} \text{s}^{-1}$ at $T \sim 0.1$ MeV, rising to $\eta \sim 10^{22} \text{g cm}^{-1} \text{s}^{-1}$ at $T \sim 0.001$ MeV (see Fig. 5 of Ref. [30]), so bulk viscosity would only dominate the damping of modes with very little shear flow. Radial pulsations [31,32] would be an interesting example to investigate. We used a rough approximation (25) to treat the photon screening; we argued (Appendix A) that this is valid to within approximately an order of magnitude, but if a more precise estimate of the bulk viscosity was required, one could improve on our treatment by replacing the approximation (25) with separate propagators for the transverse and longitudinal photons, incorporating their separate screening mechanisms [33]. It should be noted that our calculation is limited to the small-amplitude regime ($\mu_a \ll T$). If the leptonic bulk viscosity is insufficient to damp an unstable oscillation such as an r mode, then the amplitude will rise and it will be necessary to repeat our calculation in the large-amplitude (“suprathermal”) regime [34] to see whether leptonic bulk viscosity can stop the growth of the mode once it reaches a large enough amplitude.

ACKNOWLEDGMENTS

We thank Sanjay Reddy for initial discussions that led to this project. We thank Peter Shternin, Dima Yakovlev, and the anonymous referee for many helpful comments. This research was supported in part by the Offices of Nuclear Physics and High Energy

Physics of the US Department of Energy under Contracts No. DE-FG02-91ER40628 and No. DE-FG02-05ER41375.

APPENDIX A: PHOTON SCREENING

In this Appendix we discuss the adequacy of our approximation (25) for the internal photon propagator in the modified Urca process for leptons. The energy ω of the photon is $\sim T$ because all the initial and final state particles have energies within T of their Fermi energies; however, the photon three-momentum q must be large enough to move a lepton between the muon and electron Fermi surfaces, so $q \geq q_{\min}$, where $q_{\min} = p_{F,e} - p_{F,\mu}$. Thus $\omega \ll q$, and we can write the photon self-energy in the static limit where it only depends on q . There are contributions to the longitudinal and transverse self-energies from protons, electrons, and muons. If the protons are superconducting, as they are at the temperatures of interest in this paper, then they provide an additional contribution to the transverse photon self-energy. The complete expressions are

$$\begin{aligned}\Pi_L(q) &= M_{D,p}^2 \xi_L\left(\frac{q}{k_{F,p}}\right) + M_{D,e}^2 \xi_L\left(\frac{q}{k_{F,e}}\right) \\ &\quad + M_{D,\mu}^2 \xi_L\left(\frac{q}{k_{F,\mu}}\right), \\ \Pi_T(q) &= M_{D,p}^2 \xi_T\left(\frac{q}{k_{F,p}}\right) + M_{D,e}^2 \xi_T\left(\frac{q}{k_{F,e}}\right) \\ &\quad + M_{D,\mu}^2 \xi_T\left(\frac{q}{k_{F,\mu}}\right) + \Pi_p^{(sc)}(q).\end{aligned}\quad (\text{A1})$$

The Debye mass for a given species is (see, for example, Ref. [35])

$$M_D^2 = 4\pi\alpha\mu k_F, \quad (\text{A2})$$

where μ is the Fermi energy (defined relativistically, so $\mu^2 = k_F^2 + m^2$) and k_F is the Fermi momentum. The screening functions ξ_L and ξ_T in the static limit are real, and are given by

$$\begin{aligned}\xi_L(\bar{q}) &= \frac{1}{2} + \frac{1}{2\bar{q}} \left(1 - \frac{\bar{q}^2}{4}\right) \log \left| \frac{\bar{q} + 2}{\bar{q} - 2} \right|, \\ \xi_T(\bar{q}) &= \frac{1}{8} \left[1 + \frac{\bar{q}^2}{4} - \frac{1}{\bar{q}} \left(1 - \frac{\bar{q}^2}{4}\right)^2 \log \left| \frac{\bar{q} + 2}{\bar{q} - 2} \right| \right].\end{aligned}\quad (\text{A3})$$

TABLE I. Screening parameters in MeV or MeV² for a free-nucleon model of $npe\mu$ nuclear matter; μ_B is the baryon number chemical potential, and n/n_{sat} is the baryon density relative to nuclear saturation density; μ_l is the Fermi energy of the electrons and muons; q_{\min} is the lowest photon momentum that contributes to the modified Urca process; Π_L and Π_T are defined in Eq. (A1). The last three columns compare our approximate photon propagator at $q = q_{\min}$ (final column) with the photon propagator using the full screening expressions given in Appendix A.

μ_B	n/n_{sat}	μ_l	q_{\min}^2	$\Pi_L(q_{\min})$	$\Pi_T(q_{\min})$	$q_s^2 = 5\alpha\mu_l^2$	$q_{\min}^2 + \Pi_L(q_{\min})$	$q_{\min}^2 + \Pi_T(q_{\min})$	$q_{\min}^2 + q_s^2$
1056	3.164	111.1	5908	1067	55.45	450.1	6974	5963	6358
1125	6.76	167.6	1406	2150	30.13	1025	3557	1436	2431
1200	12.03	224.4	698.3	3300	65.06	1838	3999	763.4	2537
1350	26.93	328.7	304.3	5783	215	3943	6087	519.3	4247

The full expressions for photon screening by a degenerate gas of charged fermions were first obtained by Lindhard [36]. Equation (A3) was obtained from the version of Lindhard's expressions for the dielectric permittivities ε_L and ε_T given in Ref. [37], using the fact that $\Pi_L(\omega, q) = (\omega^2 - q^2)(1 - \varepsilon_L)$ and $\Pi_T(\omega, q) = \omega^2(1 - \varepsilon_T)$ [see Sec. (6.4) of Ref. [38]]. Note that ξ_L and ξ_T above are defined in the static limit, where $\omega/q \rightarrow 0$ at fixed q . Therefore, they are different from the quantities $\chi_l(x)$ and $\chi_t(x)$, which are commonly given in the literature [33,39], and are calculated at $\omega = xq$ in the limit $q \rightarrow 0$.

In our calculations of the leptonic flavor equilibration rate, we use the rough approximation $\Pi_L = \Pi_T = q_s^2$ [Eq. (25)] instead of the correct screening expressions given above. We now explain why this is a reasonable approximation.

First we discuss the longitudinal photons. Their momentum varies from q_{\min} up to $k_{F,e} + k_{F,\mu}$, but the momentum dependence of Π_T is very moderate: from Eq. (A3) we see that as \bar{q} varies from 0 to 2, ξ_L varies from 1 to $\frac{1}{2}$. In order to judge whether, for the denominator of the longitudinal photon propagator, $q^2 + q_s^2$ is a good approximation to $q^2 + \Pi_L(q)$, we use a naive free-particle model for nuclear matter. We show the results in Table I. At each value of the baryon chemical potential μ_B , the negative-charge chemical potential μ_l is determined by requiring overall electrical neutrality. This then fixes the Fermi momenta of the protons, electrons, and muons. In Table I we see that when $q = q_{\min}$ (which is where there is greatest sensitivity to the exact form of the screening), the difference between $q^2 + q_s^2$ and $q^2 + \Pi_L(q_{\min})$ is a few percent at low density, and still less than a factor of 2 at very high densities.

For the transverse photons, ξ_T varies from 0 at $q = 0$ to $\frac{1}{3}$ at $q = \infty$, so the normal-fermion contribution to the transverse screening is more important at higher momenta. The other contribution to Π_T comes from the superconducting protons, and it is more important at low momentum. At zero momentum we have Meissner screening, but as the momentum rises, the effective screening mass drops slowly: this is seen in the calculation of Ref. [33], which finds that, for $q \gg \xi^{-1}$ (where the correlation length $\xi = p_{F,p}/[m_p T_{c,p}]$), and assuming the static limit,

$$\Pi_T^{(sc)}(q) \approx \frac{\pi\alpha p_{F,p}^2 T_{cp}}{q}. \quad (\text{A4})$$

[This result follows from Ref. [33], Eq. (49), taking $\omega \rightarrow 0$ and using $Q = \pi^2$ as specified in the preceding paragraph.] In Table I we show numerical results for the naive free-nucleon model of nuclear matter. We assumed $T_{cp} = 1$ MeV (see Ref. [23], Fig. 10, and Ref. [40], Fig. 2). At the lowest allowed photon momentum $q = q_{\min}$, which is where there is greatest sensitivity to the exact form of the screening, the difference between $q^2 + q_s^2$ and $q^2 + \Pi_T^2$ is a few percent at low density, but rises to a factor of 3 at density $n/n_{\text{sat}} = 12$, and a factor of 10 at $n/n_{\text{sat}} = 27$.

We conclude that our rough approximation of using a photon self-energy $q_s^2 = 5\alpha\mu_l^2$ [Eq. (25)] gives a reasonable estimate of the in-medium photon propagator. At low densities it is accurate to within 10%. At higher densities, up to $10\times$ nuclear saturation density in the simple model of Table I, our

approximation underestimates the screening of longitudinal photons by a factor of ~ 2 and overestimates the screening of transverse photons by a factor of ~ 3 . (At even higher densities, where a description in terms of nucleons is probably no longer appropriate, our approximation for transverse screening deviates further from the free-nucleon model.) Because the rate involves the square of the photon propagator, we conclude that our approximate treatment of the photon propagator affects the rate by less than an order of magnitude at reasonable densities for nuclear matter.

APPENDIX B: PARTIAL RATE INTEGRALS

The following abbreviations are used throughout this Appendix:

$$\begin{aligned} x_m &= \frac{m_\mu}{\mu_l}, \quad x_s = \frac{q_s}{\mu_l}, \quad t = \frac{T}{\mu_l}, \\ C_{12} &= 1 - \cos \theta_2, \quad C_{14} = 1 - \sqrt{1 - x_m^2} \cos \theta_4, \\ C_{24} &= 1 - \sqrt{1 - x_m^2} [\sin \theta_2 \sin \theta_4 (\sin \phi_2 \sin \phi_4 + \cos \phi_2 \cos \phi_4) + \cos \theta_2 \cos \theta_4], \\ \bar{C}_{13} &= 1 - (1 - x_m^2) [\sin \theta_1 \sin \theta_3 (\sin \phi_1 \sin \phi_3 + \cos \phi_1 \cos \phi_3) + \cos \theta_1 \cos \theta_3], \\ \bar{C}_{14} &= 1 - (1 - x_m^2) \cos \theta_1, \quad \bar{C}_{34} = 1 - (1 - x_m^2) \cos \theta_3, \end{aligned} \quad (\text{B1})$$

$$\begin{aligned} F(x_a, x_b, x_c, x_d) &= \frac{2 \exp[(x_c + x_d - 2)/t] \{1 + 2 \exp[(x_b - 1)/t] + \exp[(x_b + x_d - 2)/t]\}}{\{1 + \exp[(x_a - 1)/t]\} \{1 + \exp[(x_b - 1)/t]\}^2 \{1 + \exp[(x_c - 1)/t]\} \{1 + \exp[(x_d - 1)/t]\}^2}, \\ I_\omega^e &= \int dx_2 dx_4 dy_1 dy_2 y_1^2 y_2^2 F(x_4 + y_1 + y_2 - x_2 + 1, x_2, 1, x_4), \end{aligned} \quad (\text{B2})$$

$$\begin{aligned} I_\omega^\mu &= \int dx_1 dx_3 dy_1 dy_2 y_1^2 y_2^2 F(x_1, 1, x_3, x_1 - x_3 - y_1 - y_2 + 1), \\ I_{d\Omega}^{e11} &= \sqrt{1 - x_m^2} \int d\Omega_2 d\Omega_4 \frac{4C_{12}C_{14} + 2C_{12}C_{24} - 2C_{14}C_{24} - 4x_m^2 C_{12} + x_m^2 C_{24}}{(x_m^2 - 2C_{24} - x_s^2)^2}, \end{aligned} \quad (\text{B3})$$

$$\begin{aligned} I_{d\Omega}^{e12} &= -\sqrt{1 - x_m^2} \int d\Omega_2 d\Omega_4 \left[\frac{-2C_{12}C_{24}^2 + 2C_{14}C_{24}^2 + 8C_{12}C_{14} + 4C_{12}C_{24} - 4C_{12}C_{14}C_{24} - 4C_{14}C_{24}}{(x_m^2 - 2C_{24} - x_s^2)^2} \right. \\ &\quad \left. + \frac{x_m^2(4C_{12}^2 - 8C_{12} + 4C_{14} + C_{12}C_{24} - C_{14}C_{24}) - x_m^4}{(x_m^2 - 2C_{24} - x_s^2)^2} \right], \end{aligned} \quad (\text{B4})$$

$$I_{d\Omega}^{e13} = -\sqrt{1 - x_m^2} \int d\Omega_2 d\Omega_4 \frac{-4C_{12}C_{14} - 4C_{12}C_{24} + 6x_m^2 C_{12}}{(x_m^2 - 2C_{24} - x_s^2)(x_m^2 - 2C_{14} - x_s^2)}, \quad (\text{B5})$$

$$\begin{aligned} I_{d\Omega}^{e14} &= \sqrt{1 - x_m^2} \int d\Omega_2 d\Omega_4 \left[\frac{2C_{12}C_{14}^2 - 4C_{12}C_{14} - 4C_{12}C_{24} + 2C_{12}C_{14}C_{24}}{(x_m^2 - 2C_{24} - x_s^2)(x_m^2 - 2C_{14} - x_s^2)} \right. \\ &\quad \left. + \frac{x_m^2(-C_{12}^2 + 6C_{12} - 2C_{12}C_{14} + 2C_{14} - 2C_{24}) + x_m^4/2}{(x_m^2 - 2C_{24} - x_s^2)(x_m^2 - 2C_{14} - x_s^2)} \right], \end{aligned} \quad (\text{B6})$$

$$I_{d\Omega}^{e22} = \sqrt{1 - x_m^2} \int d\Omega_2 d\Omega_4 \frac{4C_{12}C_{14} + 2C_{12}C_{24} - 2C_{14}C_{24} - 4x_m^2 C_{12} + 4x_m^2 C_{14} + x_m^2 C_{24} - x_m^4}{(x_m^2 - 2C_{24} - x_s^2)^2}, \quad (\text{B7})$$

$$\begin{aligned} I_{d\Omega}^{e23} &= \sqrt{1 - x_m^2} \int d\Omega_2 d\Omega_4 \left[\frac{2C_{12}C_{24}^2 - 4C_{12}C_{14} - 4C_{12}C_{24} + 2C_{12}C_{14}C_{24}}{(x_m^2 - 2C_{24} - x_s^2)(x_m^2 - 2C_{14} - x_s^2)} \right. \\ &\quad \left. + \frac{x_m^2(-C_{12}^2 + 6C_{12} - 2C_{12}C_{24} - 2C_{14} + 2C_{24}) + x_m^4 C_{12}/2}{(x_m^2 - 2C_{24} - x_s^2)(x_m^2 - 2C_{14} - x_s^2)} \right], \end{aligned} \quad (\text{B8})$$

$$I_{d\Omega}^{e24} = -\sqrt{1-x_m^2} \int d\Omega_2 d\Omega_4 \left[\frac{2C_{12}^2 C_{14} - 4C_{12} C_{14} + 2C_{12}^2 C_{24} - 4C_{12} C_{24}}{(x_m^2 - 2C_{24} - x_s^2)(x_m^2 - 2C_{14} - x_s^2)} + \frac{x_m^2(-4C_{12}^2 + 5C_{12} + C_{12} C_{14} + C_{12} C_{24} + C_{14} + C_{24})}{(x_m^2 - 2C_{24} - x_s^2)(x_m^2 - 2C_{14} - x_s^2)} \right], \quad (\text{B9})$$

$$I_{d\Omega}^{e33} = \sqrt{1-x_m^2} \int d\Omega_2 d\Omega_4 \frac{2C_{12} C_{14} + 4C_{12} C_{24} - 2C_{14} C_{24} + x_m^2(-4C_{12} + C_{14})}{(x_m^2 - 2C_{14} - x_s^2)^2}, \quad (\text{B10})$$

$$I_{d\Omega}^{e34} = -\sqrt{1-x_m^2} \int d\Omega_2 d\Omega_4 \left[\frac{-2C_{12} C_{14}^2 + 4C_{12} C_{14} + 2C_{14}^2 C_{24} + 8C_{12} C_{24} - 4C_{12} C_{14} C_{24} - 4C_{14} C_{24}}{(x_m^2 - 2C_{14} - x_s^2)^2} + \frac{x_m^2(2C_{12}^2 - 8C_{12} + C_{12} C_{14} - C_{14} C_{24} + 4C_{24}) - x_m^4}{(x_m^2 - 2C_{14} - x_s^2)^2} \right], \quad (\text{B11})$$

$$I_{d\Omega}^{e44} = \sqrt{1-x_m^2} \int d\Omega_2 d\Omega_4 \frac{2C_{12} C_{14} + 4C_{12} C_{24} - 2C_{14} C_{24} + x_m^2(-4C_{12} + C_{14} + 4C_{24}) - x_m^4}{(x_m^2 - 2C_{14} - x_s^2)^2}, \quad (\text{B12})$$

$$I_{d\Omega}^{\mu11} = (1-x_m^2)^{3/2} \int d\Omega_1 d\Omega_3 \frac{-2\bar{C}_{13}\bar{C}_{14} + 2\bar{C}_{13}\bar{C}_{34} + 4\bar{C}_{14}\bar{C}_{34} + x_m^2(3\bar{C}_{14} - 5\bar{C}_{34}) - x_m^4}{(2x_m^2 - 2\bar{C}_{13} - x_s^2)^2}, \quad (\text{B13})$$

$$I_{d\Omega}^{\mu12} = -(1-x_m^2)^{3/2} \int d\Omega_1 d\Omega_3 \left[\frac{-2\bar{C}_{13}\bar{C}_{14}^2 + 4\bar{C}_{14}^2 - 2\bar{C}_{13}\bar{C}_{34}^2 - 4\bar{C}_{34}^2 + 8\bar{C}_{13}\bar{C}_{34} + 8\bar{C}_{14}\bar{C}_{34}}{(2x_m^2 - 2\bar{C}_{13} - x_s^2)^2} + \frac{x_m^2(4\bar{C}_{14}^2 + 4\bar{C}_{34}^2 - 8\bar{C}_{13} + 2\bar{C}_{13}\bar{C}_{14} - 8\bar{C}_{14} - 2\bar{C}_{13}\bar{C}_{34} - 4\bar{C}_{14}\bar{C}_{34} - 8\bar{C}_{34})}{(2x_m^2 - 2\bar{C}_{13} - x_s^2)^2} + \frac{x_m^4(3\bar{C}_{13} - 2\bar{C}_{14} + 2\bar{C}_{34} + 10) - 3x_m^6}{(2x_m^2 - 2\bar{C}_{13} - x_s^2)^2} \right], \quad (\text{B14})$$

$$I_{d\Omega}^{\mu13} = -(1-x_m^2)^{3/2} \int d\Omega_1 d\Omega_3 \left[\frac{2\bar{C}_{13}\bar{C}_{34}^2 + 2\bar{C}_{14}\bar{C}_{34}^2 - 4\bar{C}_{13}\bar{C}_{34} - 4\bar{C}_{14}\bar{C}_{34}}{(2x_m^2 - 2\bar{C}_{13} - x_s^2)(2x_m^2 - 2\bar{C}_{14} - x_s^2)} + \frac{x_m^2(-4\bar{C}_{34}^2 + 5\bar{C}_{13} + 5\bar{C}_{14} + \bar{C}_{13}\bar{C}_{34} + \bar{C}_{14}\bar{C}_{34} + 5\bar{C}_{34})}{(2x_m^2 - 2\bar{C}_{13} - x_s^2)(2x_m^2 - 2\bar{C}_{14} - x_s^2)} + \frac{x_m^4(-3\bar{C}_{13}/2 - 3\bar{C}_{14}/2 - \bar{C}_{34} - 6) + 2x_m^6}{(2x_m^2 - 2\bar{C}_{13} - x_s^2)(2x_m^2 - 2\bar{C}_{14} - x_s^2)} \right], \quad (\text{B15})$$

$$I_{d\Omega}^{\mu14} = (1-x_m^2)^{3/2} \int d\Omega_1 d\Omega_3 \left[\frac{2\bar{C}_{13}\bar{C}_{34}^2 + 4\bar{C}_{34}^2 - 8\bar{C}_{13}\bar{C}_{34} - 8\bar{C}_{14}\bar{C}_{34}}{(2x_m^2 - 2\bar{C}_{13} - x_s^2)(2x_m^2 - 2\bar{C}_{14} - x_s^2)} + \frac{x_m^2(-\bar{C}_{14} - 3\bar{C}_{34}^2 + 6\bar{C}_{13} + 8\bar{C}_{14} + 2\bar{C}_{13}\bar{C}_{34} + 2\bar{C}_{14}\bar{C}_{34} + 8\bar{C}_{34})}{(2x_m^2 - 2\bar{C}_{13} - x_s^2)(2x_m^2 - 2\bar{C}_{14} - x_s^2)} + \frac{x_m^4(-3\bar{C}_{13}/2 - 2\bar{C}_{34} - 9) + 3x_m^6/2}{(2x_m^2 - 2\bar{C}_{13} - x_s^2)(2x_m^2 - 2\bar{C}_{14} - x_s^2)} \right], \quad (\text{B16})$$

$$I_{d\Omega}^{\mu22} = (1-x_m^2)^{3/2} \int d\Omega_1 d\Omega_3 \frac{2\bar{C}_{14}^2 - 2\bar{C}_{34}^2 + 4\bar{C}_{13}\bar{C}_{34} + 4\bar{C}_{14}\bar{C}_{34} + x_m^2(-4\bar{C}_{13} - 4\bar{C}_{34}) + 4x_m^4}{(2x_m^2 - 2\bar{C}_{13} - x_s^2)^2}, \quad (\text{B17})$$

$$I_{d\Omega}^{\mu23} = (1-x_m^2)^{3/2} \int d\Omega_1 d\Omega_3 \left[\frac{2\bar{C}_{14}\bar{C}_{34}^2 + 4\bar{C}_{34}^2 - 8\bar{C}_{13}\bar{C}_{34} - 8\bar{C}_{14}\bar{C}_{34}}{(2x_m^2 - 2\bar{C}_{13} - x_s^2)(2x_m^2 - 2\bar{C}_{14} - x_s^2)} + \frac{x_m^2(-\bar{C}_{13}^2 - 3\bar{C}_{34}^2 + 10\bar{C}_{13} + \bar{C}_{13}\bar{C}_{14} + 6\bar{C}_{14} + 2\bar{C}_{13}\bar{C}_{34} + 2\bar{C}_{14}\bar{C}_{34} + 8\bar{C}_{34})}{(2x_m^2 - 2\bar{C}_{13} - x_s^2)(2x_m^2 - 2\bar{C}_{14} - x_s^2)} + \frac{x_m^4(-\bar{C}_{13} - 2\bar{C}_{14} - 2\bar{C}_{34} - 10) + 2x_m^6}{(2x_m^2 - 2\bar{C}_{13} - x_s^2)(2x_m^2 - 2\bar{C}_{14} - x_s^2)} \right], \quad (\text{B18})$$

$$I_{d\Omega}^{\mu24} = -(1-x_m^2)^{3/2} \int d\Omega_1 d\Omega_3 \frac{4\bar{C}_{34}^2 - 8\bar{C}_{13}\bar{C}_{34} - 8\bar{C}_{14}\bar{C}_{34} + x_m^2(8\bar{C}_{13} + 8\bar{C}_{14} + 8\bar{C}_{34}) - 8x_m^4}{(2x_m^2 - 2\bar{C}_{13} - x_s^2)(2x_m^2 - 2\bar{C}_{14} - x_s^2)}, \quad (\text{B19})$$

$$I_{d\Omega}^{\mu33} = (1-x_m^2)^{3/2} \int d\Omega_1 d\Omega_3 \frac{-2\bar{C}_{14}^2 + 2\bar{C}_{14}\bar{C}_{34} + x_m^2(\bar{C}_{13} + 6\bar{C}_{14} - 3\bar{C}_{34}) - 3x_m^4}{(2x_m^2 - 2\bar{C}_{14} - x_s^2)^2}, \quad (\text{B20})$$

$$I_{d\Omega}^{\mu 34} = -(1-x_m^2)^{3/2} \int d\Omega_1 d\Omega_3 \left[\frac{2\bar{C}_{13}^2 - 2\bar{C}_{13}\bar{C}_{14}^2 + 2\bar{C}_{13}\bar{C}_{14} - 2\bar{C}_{13}\bar{C}_{34} + 2\bar{C}_{13}\bar{C}_{14}\bar{C}_{34}}{(2x_m^2 - 2\bar{C}_{14} - x_s^2)^2} + \frac{x_m^2(-\bar{C}_{13}^2 - \bar{C}_{34}^2 + 2\bar{C}_{13} + 4\bar{C}_{13}\bar{C}_{14} + 2\bar{C}_{14})}{(2x_m^2 - 2\bar{C}_{14} - x_s^2)^2} + \frac{x_m^4(-2\bar{C}_{13} - 2\bar{C}_{14} - 2) + 2x_m^6}{(2x_m^2 - 2\bar{C}_{14} - x_s^2)^2} \right], \quad (\text{B21})$$

$$I_{d\Omega}^{\mu 44} = (1-x_m^2)^{3/2} \int d\Omega_1 d\Omega_3 \frac{2\bar{C}_{13}^2 - 2\bar{C}_{34}^2 + 4\bar{C}_{13}\bar{C}_{34} + 4\bar{C}_{14}\bar{C}_{34} + x_m^2(-4\bar{C}_{14} - 4\bar{C}_{34}) + 4x_m^4}{(2x_m^2 - 2\bar{C}_{14} - x_s^2)^2}. \quad (\text{B22})$$

-
- [1] N. Andersson, *Astrophys. J.* **502**, 708 (1998).
- [2] L. Lindblom, in *Gravitational Waves: A Challenge to Theoretical Astrophysics*, ICTP Lecture Notes Series, Vol. III, edited by V. Ferrari, J. C. Miller, and L. Rezzolla (ICTP, Trieste, Italy, 2001), pp. 257–275.
- [3] B. J. Owen, L. Lindblom, C. Cutler, B. F. Schutz, A. Vecchio, and N. Andersson, *Phys. Rev. D* **58**, 084020 (1998).
- [4] P. Haensel, K. P. Levenfish, and D. G. Yakovlev, *Astron. Astrophys.* **357**, 1157 (2000).
- [5] P. Haensel, K. P. Levenfish, and D. G. Yakovlev, *Astron. Astrophys.* **372**, 130 (2001).
- [6] N. Andersson, G. L. Comer, and K. Glampedakis, *Nucl. Phys. A* **763**, 212 (2005).
- [7] D. Chatterjee and D. Bandyopadhyay, *Phys. Rev. D* **75**, 123006 (2007).
- [8] M. E. Gusakov, *Phys. Rev. D* **76**, 083001 (2007).
- [9] D. Chatterjee and D. Bandyopadhyay, *Physics and Astrophysics of Hadrons and Hadronic Matter*, edited by A. B. Santra (Narosa Publishing House, New Delhi, India), p. 237.
- [10] L. Lindblom and B. J. Owen, *Phys. Rev. D* **65**, 063006 (2002).
- [11] P. Haensel, K. P. Levenfish, and D. G. Yakovlev, *Astron. Astrophys.* **381**, 1080 (2002).
- [12] D. Chatterjee and D. Bandyopadhyay, *Astrophys. J.* **680**, 686 (2008).
- [13] J. Madsen, *Phys. Rev. Lett.* **85**, 10 (2000).
- [14] J. Madsen, *Phys. Rev. D* **46**, 3290 (1992).
- [15] B. A. Sa'd, I. A. Shovkovy, and D. H. Rischke, *Phys. Rev. D* **75**, 125004 (2007).
- [16] C. Manuel, A. Dobado, and F. J. Llanes-Estrada, *J. High Energy Phys.* **09** (2005) 076.
- [17] M. G. Alford and A. Schmitt, *J. Phys. G* **34**, 67 (2007).
- [18] B. A. Sa'd, I. A. Shovkovy, and D. H. Rischke, *Phys. Rev. D* **75**, 065016 (2007).
- [19] C. Manuel and F. J. Llanes-Estrada, *J. Cosmol. Astropart. Phys.* **08** (2007) 001.
- [20] H. Dong, N. Su, and Q. Wang, *J. Phys. G* **34**, S643 (2007).
- [21] M. G. Alford, M. Braby, S. Reddy, and T. Schafer, *Phys. Rev. C* **75**, 055209 (2007).
- [22] D. J. Dean and M. Hjorth-Jensen, *Rev. Mod. Phys.* **75**, 607 (2003).
- [23] H. Muther and W. H. Dickhoff, *Phys. Rev. C* **72**, 054313 (2005).
- [24] S. Gandolfi, A. Y. Illarionov, F. Pederiva, K. E. Schmidt, and S. Fantoni, *Phys. Rev. C* **80**, 045802 (2009).
- [25] M. Srednicki, *Quantum Field Theory* (Cambridge University Press, New York, 2007).
- [26] P. Jaikumar, C. Gale, and D. Page, *Phys. Rev. D* **72**, 123004 (2005).
- [27] A. D. Kaminker and P. Haensel, *Acta Phys. Pol. B* **30**, 1125 (1999).
- [28] V. D. Barger and R. J. N. Phillips, *Collider Physics* (Addison-Wesley, Reading, MA, 1996).
- [29] R. Mertig, M. Böhm, and A. Denner, *Comput. Phys. Commun.* **64**, 345 (1991).
- [30] P. S. Shternin and D. G. Yakovlev, *Phys. Rev. D* **78**, 063006 (2008).
- [31] M. E. Gusakov and N. Andersson, *Mon. Not. R. Astron. Soc.* **372**, 1776 (2006).
- [32] C. Cutler, L. Lindblom, and R. J. Splinter, *Astrophys. J.* **363**, 603 (1990).
- [33] P. S. Shternin and D. G. Yakovlev, *Phys. Rev. D* **75**, 103004 (2007).
- [34] P. Haensel, K. P. Levenfish, and D. G. Yakovlev, *Astron. Astrophys.* **394**, 213 (2002).
- [35] P. S. Shternin and D. G. Yakovlev, *Phys. Rev. D* **74**, 043004 (2006).
- [36] J. Lindhard, *Dan. Mat. Fys. Medd.* **28**, 3 (1954).
- [37] E. Cockayne and Z. H. Levine, *Phys. Rev. B* **74**, 235107 (2006).
- [38] M. Le Bellac, *Thermal Field Theory*. Cambridge Monographs in Mathematics and Physics (Cambridge University Press, Cambridge, UK, 1996).
- [39] H. Heiselberg and C. J. Pethick, *Phys. Rev. D* **48**, 2916 (1993).
- [40] M. Baldo and H. J. Schulze, *Phys. Rev. C* **75**, 025802 (2007).